M. Hassani-Gangaraj, D. Veysset, K. A. Nelson, and C. A. Schuh, Scripta Materialia. **145** (2018) 9-13.

# In-situ Observations of Single Micro-particle Impact Bonding

Mostafa Hassani-Gangaraj[1], David Veysset[2,3], Keith A. Nelson[2,3], Christopher A. Schuh[1]*

[1]Department of Materials Science and Engineering, MIT, Cambridge, Massachusetts 02139, USA.

[2]Institute for Soldier Nanotechnologies, MIT, Cambridge, Massachusetts 02139, USA.

[3]Department of Chemistry, MIT, Cambridge, Massachusetts 02139, USA.

*Correspondence to: schuh@mit.edu

Received 12 July 2017, Revised 25 September 2017, Accepted 26 September 2017,

Available online 12 October 2017

https://doi.org/10.1016/j.scriptamat.2017.09.042

## Abstract

We study supersonic impact of individual metallic microparticles on metallic substrates, that is, the unit process of materials buildup in cold spray coatings/additive manufacturing. We resolve the moment of impact bonding through real-time observations of single particle impacts with micron-scale and nanosecond-level resolution. We offer the first *in-situ* observation of a material-dependent threshold velocity, above which the particle undergoes an impact-induced jet-like material ejection and adheres to the substrate. We report direct measurements of critical velocities for structural metals, which unlike in nozzle experiments, are not affected by process-related complexities obscuring particles' kinetic and thermal histories.

Keywords: Cold spray, Adhesion, Additive manufacturing, Impact

## Text

Understanding material behavior under high velocity impact is the key to addressing a variety of fundamental questions in areas ranging from geological cratering [1] to impact-induced phase transformations [2], spallation [3], wear [4], and ballistic penetration [5]. Recently, adhesion has emerged in this spectrum since it has been found that micrometer-sized metallic particles can bond to metallic substrates under supersonic-impact conditions [6–11]. The phenomenon of impact-

induced adhesion of microparticles has led to the emergence of cold-spray coating, which has not only proved successful in making corrosion-, wear- and fatigue-resistant coatings [12–20], but also opened a new window in structural repair [21] and additive manufacturing [22].

In cold spray coating, researchers have repeatedly observed a "critical velocity", a threshold above which supersonic particles adhere to the substrate instead of rebounding [7,23–25]. A variety of mechanisms such as adiabatic shear instability [7], localized melting [26], viscous-type mechanical interlocking [27], interfacial restructuring or amorphization [28], and oxide-layer break-up [29] have been put forth to explain this phenomenon. Among these mechanisms, adiabatic shear instability has acquired more consensus [9,11,30–32] as it enjoyed support from Lagrangian finite element simulations [7,23], but it has not been directly observed. These mechanisms are not mutually exclusive. However, for a fixed particle/substrate materials pair and fixed processing conditions, the premise of a single critical velocity suggests that a single mechanism may dominate the binary separation between bonding and not. A cold spray deposit comprises millions of splats, each of which interacts with a carrier gas and other particles in a unique way. Each splat experiences distinct thermal and kinetic histories, impacts the deposit and is impacted by other particles in an unknown fashion. All these complexities give rise to a variety of phenomena that can potentially obscure the main phenomenon leading to bonding.

In our view, a systematic approach to focus on the unit process of material build up in cold spray, i.e., impact bonding of a single microparticle, without the complexities of nozzle experiments, is much needed for a clear understanding of bonding in cold spray. Furthermore, we attribute the lack of consensus on the operative mechanisms, in part, to a lack of real-time studies of supersonic micro-particle impact. Such studies require spatial (micron) and temporal (nanosecond) resolutions much finer than those provided by existing experimental techniques.

Here, we offer an alternative approach by conducting the first *in-situ* single-particle study of supersonic adhesion of metallic microparticles. The present letter is based on Ref. [33], and employs an in-house-designed microscale ballistic test platform to accelerate micrometer-size particles [34,35] and observe their impact behaviors in real time [36,37]. As schematically shown in Fig. 1, a laser excitation pulse is focused onto a launching pad assembly from which single metallic particles are launched toward a target sample by ablation of a gold layer and rapid expansion of an elastomeric polyurea film. The particle approach and impact on the target are observed in real time using a high-frame-rate camera and a synchronized quasi-cw laser imaging pulse for illumination. The launching pad assembly follows the design described by Lee et al. and Veysset et al. in refs [35,36]. 210-μm-thick glass substrates (Corning No. 2 microscope cover slip) were sputter-coated with a 60-nm thick gold film. A mixture of polycarbodiimide-modified diphenylmethane diisocyanate (Isonate 143L MDI, Dow Chemicals) and oligomeric diamine (Versalink® P-650, Air Products) with a weight ratio of 1:3 was spin-coated on the gold-coated substrates at 750 RPM for 5 min to yield a film thickness of 30 μm after 24-hour curing at room temperature. Film thicknesses were measured using a 3D laser scanning confocal microscope (VK-

X200 series, Keyence). Metallic particles were deposited on the substrates using lens cleaning papers to spread drops from a suspension of particles in ethanol.

For each experiment, a laser excitation pulse (pulsed Nd:YAG, 10-ns duration, 532- nm wavelength) was focused onto the launching pad assembly from where the metallic particles were ejected. Upon laser ablation of the gold film, particles were accelerated to speeds ranging from approximately 100 to 1200 m/s, controllable by adjusting the laser excitation pulse energy (from 2 up to 60 mJ). 16-image sequences showing impact were recorded with a high-frame-rate camera (SIMX 16, Specialised Imaging) using a laser pulse (30-µs duration, 640-nm wavelength SI-LUX640, Specialised Imaging) for illumination. The high-speed camera comprises 16 CCDs that can be triggered independently to record up to 16 images with exposure times as short as 3 ns.

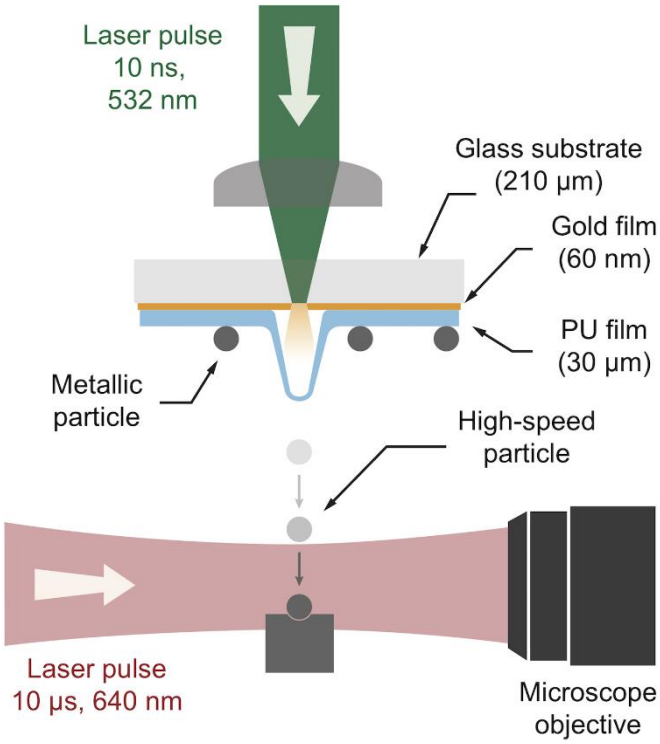


**Fig. 1.** Experimental platform for microparticle impact test and real-time imaging.

We considered four structural metals that cover a wide range of relevant cold spray applications (Al, Cu, Ni and Zn), and conducted impact experiments with matched particle and substrate materials pairs. We purchased two batches of Al powder particles with nominal particle sizes of 20 and 31 µm from Valimet (Stockton, USA). We also purchased Cu, Ni, and Zn powder particles

with nominal particle sizes of 10 μm, 5-15 μm and 6-9 μm respectively, from Alfa Aesar (Ward Hill, USA). Al, Zn, Ni and Cu plates with 3.175 mm thickness were purchased from OnlineMetals (Seattle, USA). We used a water jet cutter to extract 15 × 15 × 3.175 mm plates for use as the targets for the impact experiments. Each target surface was ground and polished to 1 μm mirror finish prior to the impact experiments.

Before each impact test, particles to be launched were selected using a secondary CCD camera. For each impact, the particle diameter was extracted from the image sequence. The measured particle diameters are 14 ± 2 and 30 ± 7 μm for Al, 10 ± 2 μm for Ni, 14 ± 2 μm for Cu and 11 ± 2 μm for Zn. We have also conducted impact experiments on larger Al particles (45 μm) to resolve the particle deformation during impact with 10 ns time intervals.

Our method resolves the instant of impact with micrometer-scale spatial resolution and nanosecond-level temporal resolution. Fig. 2a shows some exemplar results taken for a 15-μm Al particle impacting an Al target a velocity of 765 m/s (± 2%). The full-field video is available in the Supplementary information (Video S1) and has a field of view of 637 × 478 μm. At this velocity, the particle rebounded. Flattening of the particle upon impact can be noted in the $4^{th}$ and $5^{th}$ snapshots. The particle is rotating in the subsequent snapshots. The circular cross section seen in the $10^{th}$ snapshot is actually the contact area upon impact, which has been flattened such that it looks larger than the incoming particle itself (see the Supplementary Video S1). Fig. 2b shows another example taken for a 16-μm Al particle impacting an Al target a higher velocity of 825 m/s (± 2%). This particle got flattened upon impact (the $4^{th}$ snapshot). Particles tested at higher impact velocities did not rebound, but instead adhered to the substrate; these impact velocities exceeded the critical velocity (see Supplementary Video S2).

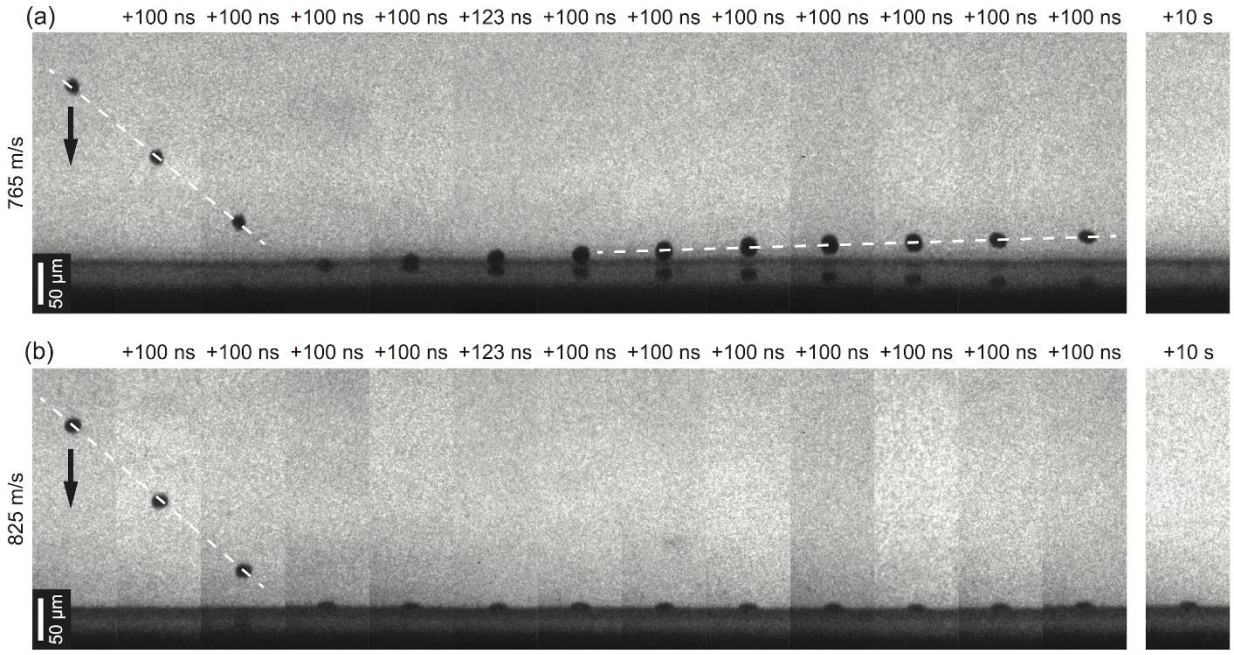


**Fig. 2.** In situ observation of microparticle supersonic impact. Multi-frame sequences with 5 ns exposure time showing a single Al particle impacting on an Al substrate. (a) The microparticle arrives from the top of the field of view with a speed of 765 m/s, impacts the substrate and subsequently rebounds with a speed of 35 m/s. (b) The microparticle impacts the substrate with a speed of 825 m/s and subsequently adheres to the surface. The relative delay from the initial image is shown at the top of each frame. The images are cropped from their original size to show the region of interest (see Supplementary Videos S1-2 for a full-field view).

Processing images such as those in Fig. 2a and b leads to data such as shown in Fig. 3, where the coefficient of restitution, defined as the ratio between the rebound velocity and the impact velocity, is shown as a function of impact velocity for four materials. As the impact velocity increases, the coefficient of restitution decreases until it eventually goes to zero, separating the two regimes of rebound and bonding, and revealing the critical velocity for adhesion. Our method has therefore enabled the first direct measurements of critical adhesion velocity for Cu, Ni, Al and Zn particles to matched-material substrates (see Table 1 for numerical values).

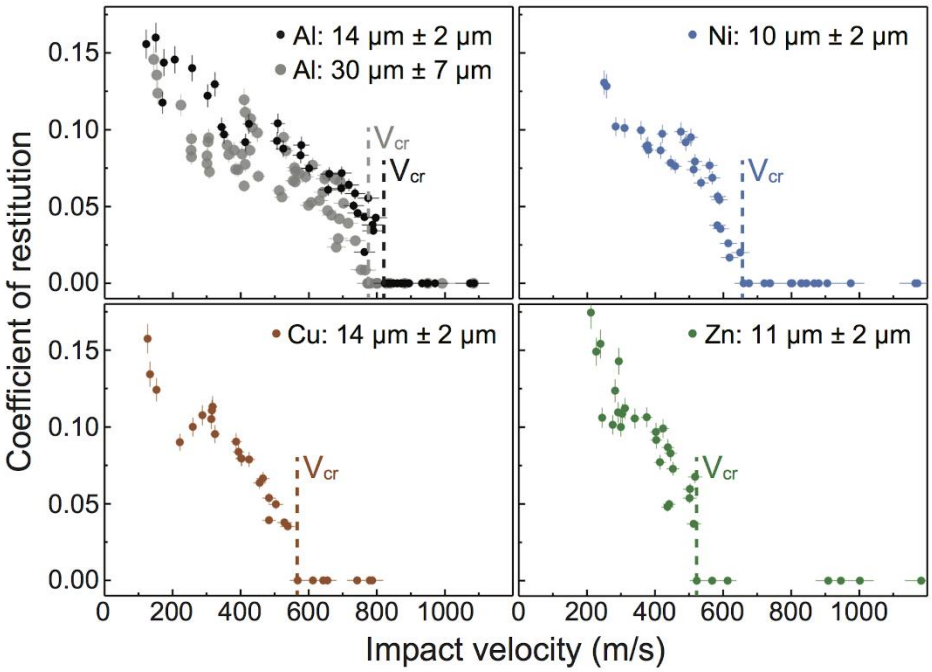


**Fig. 3.** Coefficient of restitution for Al, Ni, Cu, and Zn. The coefficient of restitution is equal to zero above the critical velocity.

**Table 1.** Critical velocity ranges for Al, Ni, Cu, and Zn. The lower bound corresponds to the highest velocity at which rebound was observed and the higher bound the lowest velocity at which adhesion was observed. The uncertainty on the velocity measurement is 2%.

| Material | Critical velocity (m/s) |
|---|---|
| Aluminum | [797-824] |
| Nickel | [650-660] |
| Copper | [539-568] |
| Zinc | [518-523] |

Prior to this work, the critical velocity has been always determined in full cold spray coating experiments or wipe tests in a semi-empirical fashion [38]. That is, particle velocity distributions for a given nozzle, a given material and a given set of processing conditions (stagnation pressure and temperature) are calculated using computational fluid dynamics [39]. The velocity distribution is then combined with the measured deposition efficiency and the particle size distribution, to give the size and velocity of the largest particle which would bond successfully to the substrate [7]. The

calculated velocity for the largest and thus slowest [38] bonded particle is considered to be the critical velocity. The computed velocities in this approach could be considered first order approximations, as complexities such as interactions of the particles with the hot carrier gas or with one another, and the bow shock effect in front of the substrate, are overlooked. In other words, the real kinetic and thermal histories of the particles are not unambiguously known in nozzle experiment determinations of the critical velocity. Conversely, in our data in Fig. 3 we observe a clear discontinuity in the coefficient of restitution of isolated and well characterized particles at the critical velocity, following its roughly linear decline at lower velocities. Ours are therefore direct measurements of the critical velocity rather than a backed-out estimation of it.

Our method of measuring the critical velocity is also sensitive to the particle size. Figure 3 shows the data gathered using larger Al particles impacting Al substrates. Our measurements confirm a shift in critical velocity from 810 m/s for 14-µm particles to 770 m/s for 30-µm Al particles. This result is consistent with the accepted notion that larger particles should have lower critical velocities. However, calibration of a typical power relation between the critical velocity and particle size ($V_{cr} \propto d_p^n$) based on the current measurements yields to $n$=*-0.07*, which is less than typical exponent values reported for copper and stainless steel in literature [38] by a factor of two. We can attribute this to the fact that the size effect is exclusively isolated and studied in our setup, whereas accelerating particles of different sizes in cold spray nozzles introduces undesired temperature effects into the problem too; particles of different sizes heat up to different temperatures. In the present experiments, on the other hand, both 14- and 30-µm particles impact the substrates at the same temperature.

In addition to providing a clean measurement of the critical velocity, the discontinuity in the CoR plots also suggests the emergence of a physical phenomenon governing adhesion at critical and above-critical impact velocities. To capture the origin of the sudden drop—rather than the gradual decrease—in the CoR at the critical velocity, we decreased the inter-frame time between each snapshot by an order of magnitude. This allowed us to resolve the bonding moment in our in-situ experiments. Greater insight is accordingly provided by the image series in Fig. 4a and b where the interactions of slightly sub-critical (605 m/s) and slightly above-critical (805 m/s) particles with the substrates during contact are captured in multiple snapshots. The sub-critical particle (Fig. 4a) undergoes significant plastic deformation upon impact from a full sphere to an asymmetric oblate shape, and eventually rebounds. Our in-situ observation suggests that the plastic deformation is almost entirely accumulated in the lower half of the particle leaving the upper half virtually intact. Significant plastic deformation in the above-critical velocity particle (Fig. 4b) is accompanied by very fast lateral jet-like material ejection, denoted by white arrows at the periphery of the particle. This particle with the jet-like material ejection and fragmentation does not rebound. These images, also montaged into Supplementary Videos S3 and S4, are the first direct observations of the rebound-adhesion transition, and of material ejection upon an adhesive impact.

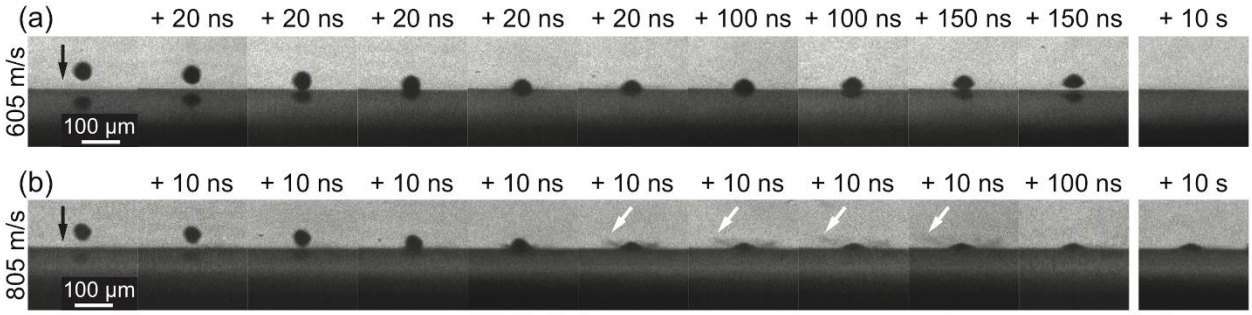


**Fig. 4.** In-situ observation of the bonding moment in microparticle impact. Multi-frame sequences with 5 ns exposure times showing 45-µm Al particle impacts on Al substrate at 605 m/s (top) and 805 m/s (bottom), respectively below and above critical velocity. The micro-projectiles arrive from the top of the field of view (see Supplementary Videos S3-4 for a full-field view). Material jetting is indicated with white arrows.

Our *in-situ* observations are in line with the post-mortem observations of material jets [40,41] in bonded particles and emphasize the importance of jetting and plastic ejection of material to obtain conditions for bonding. Large plastic deformation, caused by such jetting, could provide fresh metallic surfaces and facilitate pristine atomic contact between particle and substrate leading to bonding in cold spray [7,8], as it does in a similar manner for explosive welding [42]. Jetting and subsequent material fragmentation, however, have not previously been directly observed at the individual particle level on the time scale of the impact event itself. Our real time observations of the moment of bonding suggests that jet formation and subsequent material fragmentation is triggered at the critical impact velocity, and that this is directly associated with adhesion.

In some of our future work we will explore conditions for material jetting in more detail. Here we note that such jetting is well known in fluid drops, and physical similarity suggests exploration of that phenomenon as a starting point [43,44]. For either a fluid or a solid, conservation of volume requires that the contact periphery of the particle is laterally accelerated to a given velocity during the contact of the particle with the substrate. This lateral velocity of the contact edge is initially high (theoretically infinite at the first moment of contact), even higher than the velocity of the shock wave that is generated upon impact. The shock front, accordingly, remains initially attached to the leading edge. However, as the lateral velocity of the leading edge drops below the shock wave velocity, a release wave is reflected back into the particle exposing a local region to extreme tension and leading to jet formation and subsequent fragmentation.

To summarize, our nanosecond and microscale in-situ observations of metallic microparticle impacts have provided an alternative approach to study impact bonding in cold spray. By offering first-hand measurements of critical velocity for four structural metals, we propose a new direction of focus: studies of the unit-process of material buildup in cold spray to better understand impact bonding. For the first time, we resolved the moment of impact bonding for metallic microparticles with our *in-situ* experiments and observed jetting and local material ejection during bonding. Single particle studies should prove useful for the understanding of impact-induced adhesion across a range of materials, as well as for the design of cold spray coatings and additive manufacturing processes that rely on impact bonding.

## ACKNOWLEDGEMENTS

This research was supported by the U.S. Army Research Office under contract W911NF-13-D-0001. Support for equipment was also provided through the Office of Naval Research DURIP Grant No. N00014-13-1-0676. The authors acknowledge insightful conversations with Victor Champagne. MHG and DV thank Steve Kooi, Alex Maznev and Cyril Williams for valuable discussions. DV thanks Dmitro Martynowych for assistance in launching pad preparation. MHG thanks Atieh Moridi for valuable discussions.

## REFERENCES

[1] M.C. Malin, K.S. Edgett, L. V Posiolova, S.M. McColley, E.Z.N. Dobrea, Science 314 (2006) 1573–1577.

[2] M.D. Knudson, M.P. Desjarlais, D.H. Dolan, Science 322 (2008) 1822–1825.

[3] M.A. Meyers, C. Taylor Aimone, Prog. Mater. Sci. 28 (1983) 1–96.

[4] A.A. Voevodin, R. Bantle, A. Matthews, Wear 185 (1995) 151–157.

[5] M.E. Backman, W. Goldsmith, Int. J. Eng. Sci. 16 (1978) 1–99.

[6] A. Papyrin, V. Kosarev, S. Klinkov, A. Alkhimov, V.M. Fomin, Cold Spray Technology, Elsevier Science, 2006.

[7] H. Assadi, F. Gärtner, T. Stoltenhoff, H. Kreye, Acta Mater. 51 (2003) 4379–4394.

[8] R.C. Dykhuizen, M.F. Smith, D.L. Gilmore, R.A. Neiser, X. Jiang, S. Sampath, J. Therm. Spray Technol. 8 (1999) 559–564.

[9] V.K. Champagne, The Cold Spray Materials Deposition Process: Fundamentals and Applications, Woodhead, 2007.

[10] A. Moridi, S.M. Hassani-Gangaraj, M. Guagliano, M. Dao, Surf. Eng. 30 (2014) 369–395.

[11] H. Assadi, H. Kreye, F. Gärtner, T. Klassen, Acta Mater. 116 (2016) 382–407.

[12] S. Dosta, M. Couto, J.M. Guilemany, Acta Mater. 61 (2013) 643–652.

[13] E. Sansoucy, P. Marcoux, L. Ajdelsztajn, B. Jodoin, Surf. Coatings Technol. 202 (2008) 3988–3996.

[14] S.M. Hassani-Gangaraj, A. Moridi, M. Guagliano, Surf. Eng. 31 (2015) 803–815.

[15] H. Koivuluoto, G. Bolelli, L. Lusvarghi, F. Casadei, P. Vuoristo, Surf. Coatings Technol. 205 (2010) 1103–1107.

[16] A. Moridi, S.M. Hassani-Gangaraj, S. Vezzú, L. Trško, M. Guagliano, Surf. Coatings Technol. 283 (2015) 247–254.

[17] K. Spencer, M.-X. Zhang, Scr. Mater. 61 (2009) 44–47.

[18] H.-K. Kang, S.B. Kang, Scr. Mater. 49 (2003) 1169–1174.

[19] Y. Xie, S. Yin, C. Chen, M.-P. Planche, H. Liao, R. Lupoi, Scr. Mater. 125 (2016) 1–4.

[20] X.-T. Luo, G.-J. Yang, C.-J. Li, K. Kondoh, Scr. Mater. 65 (2011) 581–584.

[21] V.K. Champagne, D.J. Helfritch, Surf. Eng. 30 (2014) 396–403.

[22] Y. Cormier, P. Dupuis, B. Jodoin, A. Corbeil, J. Therm. Spray Technol. 25 (2016) 170–182.

[23] M. Grujicic, C.L. Zhao, W.S. DeRosset, D. Helfritch, Mater. Des. 25 (2004) 681–688.

[24] J. Wu, H. Fang, S. Yoon, H. Kim, C. Lee, Scr. Mater. 54 (2006) 665–669.

[25] T. Schmidt, H. Assadi, F. Gärtner, H. Richter, T. Stoltenhoff, H. Kreye, T. Klassen, J. Therm. Spray Technol. 18 (2009) 794–808.

[26] G. Bae, S. Kumar, S. Yoon, K. Kang, H. Na, H.-J. Kim, C. Lee, Acta Mater. 57 (2009) 5654–5666.

[27] M. Grujicic, J.R. Saylor, D.E. Beasley, W.S. DeRosset, D. Helfritch, Appl. Surf. Sci. 219 (2003) 211–227.

[28] K.H. Ko, J.O. Choi, H. Lee, Mater. Lett. 175 (2016) 13–15.

[29] W.-Y. Li, C.-J. Li, H. Liao, Appl. Surf. Sci. 256 (2010) 4953–4958.

[30] J. Villafuerte, Modern Cold Spray: Materials, Process, and Applications, Springer International Publishing, 2015.

[31] R.G. Maev, V. Leshchynsky, Cold Gas Dynamic Spray, CRC Press, 2016.

[32] C.M. Kay, J. Karthikeyan, A.S. for Metals International, High Pressure Cold Spray: Principles and Applications, ASM International, 2016.

[33] M. Hassani-Gangaraj, D. Veysset, K.A. Nelson, C.A. Schuh, arXiv:1612.08081 (2016).

[34] J.-H. Lee, D. Veysset, J.P. Singer, M. Retsch, G. Saini, T. Pezeril, K.A. Nelson, E.L. Thomas, Nat. Commun. 3 (2012) 1164.

[35] J.-H. Lee, P.E. Loya, J. Lou, E.L. Thomas, Science 346 (2014) 1092–6.

[36] D. Veysset, A.J. Hsieh, S. Kooi, A.A. Maznev, K.A. Masser, K.A. Nelson, Sci. Rep. 6 (2016) 25577.

[37] D. Veysset, A.J. Hsieh, S.E. Kooi, K.A. Nelson, Polymer (Guildf). 123 (2017) 30–38.

[38] T. Schmidt, F. Gärtner, H. Assadi, H. Kreye, Acta Mater. 54 (2006) 729–742.

[39] T. Stoltenhoff, H. Kreye, H.J. Richter, J. Therm. Spray Technol. 11 (2002) 542–550.

[40] M.V. Vidaller, A. List, F. Gaertner, T. Klassen, S. Dosta, J.M. Guilemany, J. Therm. Spray Technol. 24 (2015) 644–658.

[41] P.C. King, C. Busch, T. Kittel-Sherri, M. Jahedi, S. Gulizia, Surf. Coatings Technol. 239 (2014) 191–199.

[42] B. Crossland, Explosive Welding of Metals and Its Application, Oxford: Clarendon Press, 1982.

[43] J.E. Field, J.P. Dear, J.E. Ogren, J. Appl. Phys. 65 (1989) 533.

[44] M. Rein, Fluid Dyn. Res. 12 (1993) 61–93.